Statistical studies of Conductance Fluctuations in Quantum Dots

Rina Dutta [a]
[a] Department of Basic Science and Humanities,
University of Engineering and Management (UEM),
B/5, Plot No.III, Action Area-III, Newtown, Kolkata 700156

A mathematical formulation of the mesoscopic fluctuations of the conductance in almost closed quantum dots (weak dot-leads coupling) is discussed by RMT (Ranom Matrix Theory) as a statistical tool. A quantum dot (artificial atom) is a sub-micron-scale conducting device containing up to several thousand electrons. Transport of electron through a quantum dot at low temperatures is a quantum-coherent process. Conductance fluctuations of an arbitrary shape dot, with or without disorder, in presence/ absence of electron-electron interactions have been studied analytically. These fluctuations can be expressed in terms of the eigenfunctions of the Hamiltonian of the dots expressed in the basis of the connecting leads. The distribution of the eigenfunctions is obtained by using multiparametric Gaussian random matrix ensemble with independent matrix elements to model the non-interacting cases and the correlated Gaussian ensembles for the interacting cases.

PACS numbers:

I. INTRODUCTION

Recent developments of nanoscience makes possible to fabricate nearly isolated islands of two-dimensional electron gas on the surface of high-mobility semiconductor heterostructures[10,11]. These small conducting devices known as quantum dots can contain several thousand electrons confined to a region with linear size varying from a few nanometer to micrometer (length scale of de-Broglie wavelength). The dot easily connects to electrodes and is expected to have an irregular shape due to fluctuations in the electrostatic confinement potential. The energy levels are quantized due to three dimensional spatial confinement of electron in quantum dots.

A typical quantum dot is a mesoscopic system (van Kampen (1981)[1]), which is intermediate between a microscopic system (e.g. nuclei, atoms) and macroscopic bulk matter[4]. In a mesoscopic system, the electron's phase coherence length L_ϕ is larger than or comparable to the system's size L, where phase coherence length is the distance the electron travels without loosing its phase coherence (due to scattering etc.). The length L_ϕ increases rapidly with decreasing temperature, for $L = 1$ μm (open system), becomes mesoscopic for temperatures below 100 mK. In the mesoscopic regime, the description of transport in terms of local conductivity breaks down and the whole sample behave almost as a single coherent entity. This coherence has a strong influence on the physical properties of the sample.

Quantum coherence, in a mesoscopic sample, leads to the interference of waves describing an electron propagating along different paths between the incoming and outgoing leads. Interference effects lead to sample to sample, reproducible fluctuation of the physical properties. For example, the conductance in a metallic mesoscopic conductor shows fluctuation of the order of e^2/h, independent of the size of the average conductance; this phenomenon is known as universal conductance fluctuations[16,17]. Interference effects can also be observed in various physical properties of a given sample e.g. conductance by changing phase-sensitive parameter (e.g Fermi momentum or the external magnetic field) in the system. Another important signature of quantum coherence is the weak localization effect. This, originating in the constructive interference of the forward and time-reversed paths of the electron, affects the average transport behavior of the sample if the time-reversal symmetry is preserved. For example, the average quantum conductance is smaller in the absence of a magnetic field than in its presence. The weak localization effect requires $L_\phi \gg l$ and occurs in macroscopic conductors ($L > L_\phi$).

In a mesoscopic structure, the basic scales related to the physical properties are based on the nature of the electron dynamics, diffusive or ballistic. The relevant length scales in the disordered systems are the mean free path l, Fermi wavelength λ_F and the localization length ζ (the length over which the electron's wave function is localized). For example, the sample with $l \ll L$ corresponds to the diffusive regime, and the cases with $\lambda_F \ll l$ or $\zeta \gg l$ correspond to the metallic regime etc. The important energy scales are the Fermi energy E_F, the mean level spacing Δ and the Thouless energy $E_c = \hbar/\tau_D$; here τ_D is the characteristic time scale for the electron to diffuse across the length L of a disordered sample.

A disordered, impurity-rich quantum dot due to its diffusive regime has been an original focus of mesoscopic physics. However quantum dots are not only miniature structures whose transport properties have been measured. Similar experiments have been performed recently on smaller structures such as very clean metallic nanoparticles[6,7] C_{60} molecules deposited on gold substrate[8] and carbon nanotubes[9,15]. Some of the phenomena have been seen in these systems are similar to those observed in quantum dots, this suggest that quantum dots are generic systems for exploring the physics of small, coherent quantum structures.

II. TYPES OF QUANTUM DOTS

Quantum dots are man-made structures to be governed by the laws of quantum mechanics. The dots are made by forming a two-dimensional electron gas in the interface region of a semiconductor heterostructure and applying an electrostatic potential to metal gates to further confine the electrons to a small region in the interface plane. Since the electronic motion is restricted in all three dimensions, a quantum dot is referred to as a zero-dimensional system. The transport properties[5] of a quantum dot can be measured by coupling it to leads and passing current through the dot. The advantage of these artificial systems is that their transport properties are measured with the strength of the dot-lead couplings, number of electrons in the dot, the dot's size and shape all under experimental control. Based on transport properties, the quantum dots can basically be divided into three main types.

(i) Ballistic dot: Transport in a ballistic quantum dot is dominated by electronic scattering, not from impurities, but from the structure's boundaries. The multiple scattering from the irregular shape boundaries, before electron escapes through the dots, leads to a mostly chaotic electrons dynamics. However the fluctuations of the gate-voltage may change the confinement shape to a non-chaotic type. The nature of the underlying classical dynamics manifests itself in the quantum behavior, through localization or spreading of the wave-packets and the degree of randomization of the relevant operators. This requires $\tau_{escape} \gg \tau_c$, τ_{escape} is the mean escape time of the electron into the leads. These dots are the main focus of most experimental research on quantum dots.

(ii) Open dot: In an open dot the coupling between a quantum dot and its leads is strong and the movement of electrons across the dot-lead junction is classically allowed. In open dots with many open channels the average conductance is large and electron-electron interaction is neglected for statistical fluctuations studies. Although electron-electron inelastic scattering reduces the coherence time of the electrons at finite temperature but the excitations around the Fermi energy can safely be assumed to be noninteracting quasiparticles (Y. Alhassid, 2000). The properties of these dots can therefore be studied within Fermi liquid models.

(iii) Closed dot: In a closed dot the point contacts of the dot-lead junctions are pinched off, effective barriers are formed and the transport occurs only by quantum tunneling. As a consequence, the electron-electron interactions significantly influence the physical properties. For example, the electron in the incoming lead is repulsed by the electron already present in dot which in turn affects the conductance. This also results in quantization of the charge on the dot. The dots low-lying energy level are discrete with widths smaller than their spacings; due to this discreteness of the excitation spectra, the closed dots are also called artificial atoms[13,14].

According to geometry, there are two types of quantum dots:

(i) Lateral dot: Here current flows within the plane of the dot to which the electrons are confined. Many of the lateral dots with $N \geq 50$ electrons have no particular symmetry. Scattering of an electron from the irregular boundaries of such dots shows the single-particle dynamics that are mostly chaotic.

(ii) Vertical dot: In this dot, current flows perpendicular to the plane of the dot to which the electrons are confined. Vertical dots are suitable for spectroscopic studies of a dot with few electrons ($N \leq 20$). Such dots can be prepared in regular shapes, such as disk, where the confining potential is harmonic and the single-particle levels are arranged in shells. This shell structure is observed by measuring the Coulomb-blockade peaks as a function of the number of electrons in the dot[18].

Quantum dots can be fabricated by molecular-beam epitaxy in which a layer of AlGaAs is grown on the top of a layer of GaAs. FIG. 1 illustrate the quantum dot device fabrication. FIG. 1(a) (a quantum dot used by Fock *et al.* 1996) indicate that the electrons are trapped vertically in the interface of a GaAs/AlGaAs heterostructure and form a two dimensional electron gas (darker area). Their lateral confinement to the dot region is achieved by applying a negative voltage to the top metal gate (lighter shade), depleting the electrons underneath. The metal gates are created by electron-beam lithography process at the top of the structure. The dot is coupled to the bulk two dimensional electron-gas regions by two individually adjustable point contacts (source and drain). A voltage V_{sd} is applied between the source and drain drives a current I through the device. The linear conductance can then be defined by $G = \frac{I}{V_{sd}}$. The shape and the size of the dot can be controlled by voltages V_{g1} and V_{g2} applied to shape distorting gates. FIG. 1(b) shows the micrograph of another dot by Oosterkamp *et al.* 1997. The darker area indicates the dot region (center) and the two large two-dimensional electron-gas areas on the left and the right (source and drain regions). The lighter shade represents the metal gates. The dot's size is controlled by the middle pair of gates, and its tunnel barriers can be varied by the pairs of gates on the left and on the right. Different interesting physical situations can be observed by controlling the dot's shape, dot's area and dot-lead couplings. The confined electrons are typically 50-100 nm below the surface. To observe the charge quantization in the dot, two conditions must be satisfied; firstly, the barriers must be large enough so that the transmission is small, this gives the condition $G \ll e^2/h$. It means that the dot is almost isolated. Secondly, the temperature must be low enough so that the effects of charge quantization are not washed out. Here $KT \ll e^2/C$ is always satisfied at low temperature.

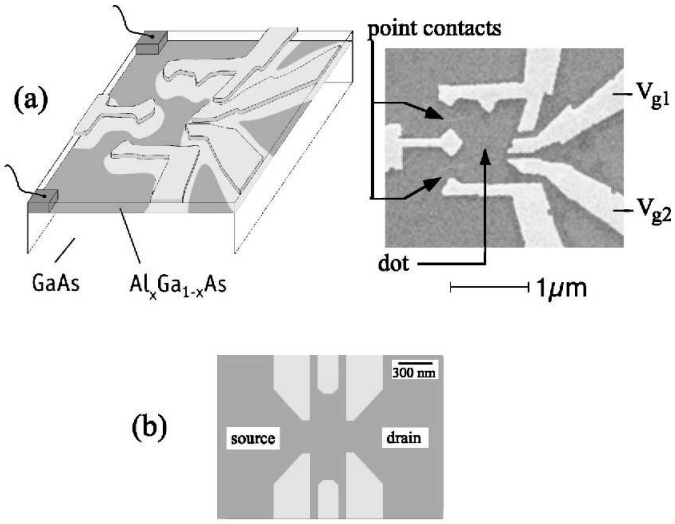

FIG. 1: Quantum dots: (a) A scanning electron micrograph of the dot (on the right, top view representation and on the left, a schematic drawing of the device). (b) A micrograph of another dot.

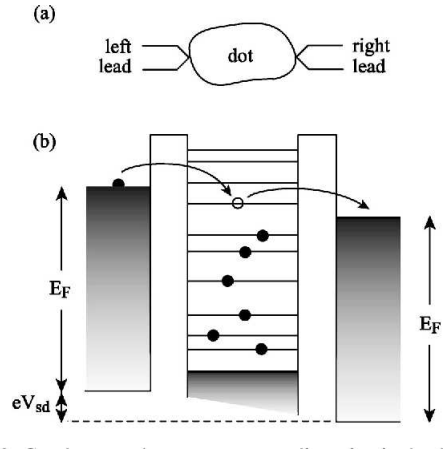

FIG. 2: Single-electron resonant tunneling through a quantum dot: (a) An isolated quantum dot with left and right leads. (b) Conductance by resonant tunneling.

III. COULOMB-BLOCKADE PHENOMENA

The tunneling[5] of an electron into the dot is blocked by the classical coulomb repulsion of the electrons already in the dot, so the conductance is small. This phenomenon, known as coulomb-blockade, occurs when an island of electrons is weakly coupled to two leads via tunnel junctions. When the coupling is weak, the conductance drops below e^2/h and the charge on the island becomes quantized. In coulomb-blockade region, the tunneling occurs through a single resonance in the dot. By changing the gate voltage V_g, coulomb repulsion can be compensated. With an appropriate value of V_g, the charge on the dot will fluctuate between N and $N+1$ electrons which leads to the maximum conductance. This phenomenon is known as resonance. The conductance then shows a series of sharp peaks as a function of the gate voltage. The period of these oscillations corresponds to the addition of a single electron to the island. This phenomenon, known as coulomb-blockade oscillation, was first observed in the metallic grains[19], where $KT \ll \Delta \ll e^2/C$. FIG. 2(a) is a schematic view of an coulomb-blockade quantum dot that is weakly coupled to left and right leads. This point contacts create a tunnel barrier between the dot and the leads. FIG. 2(b) indicate the side view of quantum dot, when the Fermi energy of the electron and the source and drain reservoirs matches the unoccupied level in the dot, the electron can tunnel across the barrier into the dot. A current will flow in response to a small source-drain voltage V_{sd}. The potential in the dot is controlled by gate voltage V_g which can be varied to observe the coulomb-blockade oscillations in the conductance.

Coulomb-blockade is a central phenomenon in closed quantum dots with large tunnel barriers. It is usually a classical phenomenon, observed at temperatures that are small compared with the charging energy. The discreteness of the dot's levels becomes important in the quantum coulomb-blockade regime when the temperature drops below mean level spacing Δ. The experimental analysis of these levels can be carried out by measuring conductance versus gate voltage (which varies the electron density and hence the fermi energy).

The coulomb interaction plays an important role in almost closed dots and can lead to an appreciable reconstruction of electronic states and to a strong suppression of the tunneling. However, for a large system, the coulomb interaction is reduced primarily due to the charging effect and can be incorporated in theory as a background potential[23,24]. In this regime, statistical properties of the conductance are mainly determined by nature of the dynamics (chaotic or near-integrable) of non-interacting electrons in a dot. The first work concerning the statistical properties of the conductance of dots has been done by Jalabert[23], who studied the conductance fluctuations caused by a single level tunneling in the situation when the external contacts are symmetric. They considered quantum billiard with chaotic dynamics of electrons, assumed that in this case fluctuations of level width are described by the Porter-Thomas Distribution[25] and checked the validity of the approach by numerical simulation. The Porter-Thomas Distribution of level widths leads to the conductance fluctuations independent of the dot's geometry, although they do depend on the properties of the leads (such as the number of modes and the average transparency in each mode).

The rms fluctuations of the conductance in a mesoscopic conductor are of the order of e^2/h, independent of the size of the average conductance. This phenomenon known as **universal conductance fluctuations**[16,17]. The link between universal conductance fluctuations in disordered systems and RMT (Random Matrix Theory) was first described by Altshuler and Shklovskii[20] and

by Imry[21]. Thouless had pointed out that there is a close connection between the conductance and spectral properties[22], the conductance expresses the sensitivity of the energy levels to a change in the boundary conditions. This relation was used by Altshuler and Shklovskii (1986) to argue that RMT spectral correlations are at the origin of the universal conductance fluctuations.

IV. RESONANCE TUNNELING

Quantum tunneling is a microscopic phenomenon where a particle can penetrate and in most cases pass through a potential barrier. The quantum dot is weakly coupled to source and drain leads and a gate voltage V_g can control its electrostatic potential. The total classical electrostatic energy of a coulomb island with N electrons is

$$\begin{aligned} U(N) &= -QV_{ext} + Q^2/2C \\ &= -NeV_{ext} + N^2e^2/2C \end{aligned} \tag{1}$$

where V_{ext} is the potential difference between the electron gas and the reservior (due to gate voltage) and C is the total capacitance between the island and its surroundings. The number of electrons in the dot for a given V_{ext} is determined by minimizing $U(N)$. We define $Q_{ext} = CV_{ext}$. When $Q_{ext} = Ne$, the minimum is obtained for the state with charge $Q = Ne$ and the energy of the state with $Q = (N \pm 1)e$ is higher by $e^2/2C$ which results the tunneling density of states has a gap of $E_c = e^2/C$ around the fermi energy, blocking the flow of electrons into the island. FIG. 3(a, c) represents the above situation. When the gate voltage tuned to a value $e\alpha V_g = Ne^2/C$ [FIG. 3(a)], there is a charging energy gap in the single-particle spectrum on both sides of the fermi energy, blocking the tunneling of electrons into the dot. But when the gate voltage changes to $e\alpha V_g = (N + 1/2)e^2/C$ [FIG. 3(b)], it compensates for the coulomb repulsion, and the charging energy for adding an electron to the dot vanishes. When the fermi energy in the leads matches the first unoccupied single-particle state in the dot, resonant tunneling of an electron into the dot occurs. FIG. 3(c) and FIG. 3(d) show the total electrostatic energy $U(N)$ of the dot vs the number of electrons: (c) for $e\alpha V_g = Ne^2/C$, the energy of the dot is minimum for N electrons in the dot, leading to charge quantization, (d) for $e\alpha V_g = (N + 1/2)e^2/C$, the energies of a dot with N and $N + 1$ electrons are equal and the dot's charge can fluctuate between Ne and $(N+1)e$. This is known as degeneracy.

The tunneling spectroscopy of quantum dots is done by measuring conductance versus gate voltage (which varies the electron density and hence the fermi energy E_F). In the weak-coupling limit, a typical resonance width in the dot is much smaller than the average spacing Δ between resonances. In this limit, only the resonance E_k that is closest to the scattering energy E contributes to the scattering matrix, thus leading to its Breit-Wigner resonance

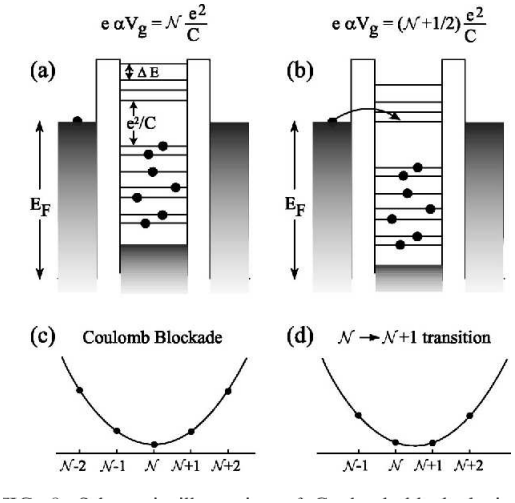

FIG. 3: Coulomb Blockade and Resonant Tunneling.

formulation[5]. The latter along with Landauer's formula for the conductance then gives the zero-temperature conductance in the tunneling regime (removing spin degeneracy),

$$G(E) = \frac{e^2}{h}\frac{\Gamma_k^l\Gamma_k^r}{(E-E_k)^2 + (\Gamma_k/2)^2} \tag{2}$$

where $\Gamma_k^{l(r)} = \sum_{c\epsilon l(r)}\Gamma_{ck}$ is the width of the level E_k to decay into left (right) lead. The finite temperatures conductance can be obtained from Eq.(2) by convoluting it with the derivative $f' = \frac{\partial f}{\partial E}$ of the Fermi-Dirac distribution. In low temperature regime $\overline{\Gamma} \ll T \ll \Delta$, f' is almost unchanged over the resonance width $\overline{\Gamma}$. G can then be approximated as

$$G(E_F, T) \approx G_k^{\text{peak}}\frac{1}{\cosh^2(\frac{E_k - E_F}{KT})} \tag{3}$$

with E_F as the fermi energy in the leads and

$$G_k^{\text{peak}} = \frac{e^2}{h}\frac{\pi\overline{\Gamma}}{4KT}g_k, \qquad g_k = \frac{2}{\overline{\Gamma}}\frac{\Gamma_k^l\Gamma_k^r}{\Gamma_k^l + \Gamma_k^r} \tag{4}$$

The Eq.(4) describes a conductance peak of width $\sim KT$, centered at $E_F = E_k$ and with a peak-height amplitude of G_k^{peak}. Here $\Gamma_k^l(r) = \sum_c |\gamma_{ck}^{l(r)}|^2$ with $\gamma_{ck}^{l(r)}$ as the partial width amplitude to decay into channel c in the left (right) lead. The quantity $\gamma_{ck}^{l(r)}$ can be expressed as a scalar product of the resonance wave function $\psi_k = (\psi_{1k}, \psi_{2k}, .., \psi_{Nk})$ and channel wave function $\phi_c = (\phi_{1c}, \phi_{2c}, ..)$:

$$\gamma_{ck} = \langle\phi_c|\psi_k\rangle$$

The partial-width amplitudes in a continuous basis can be written as

$$\gamma_{ck} = \sqrt{(\hbar^2\ k_c\ P_c/m)}\int_C dl\ \phi_c^*\ \psi_k \tag{5}$$

where P_c is the penetration factor to tunnel through the barrier in channel c, $P_c = 1$ in absence of the barrier and $P_c \ll 1$ in the presence of the barrier. The penetration factor is a smooth function of the fermi energy (or gate voltage), and fluctuations can only arise from the overlap integral, that is, the spatial fluctuations of ψ_k across the dot-lead interface. The scalar product in Eq.(5) is defined over the dot-lead interface and differs from the scalar product in the Hilbert space of the dot.

When $T \ll \Delta$, conductance is possible only by resonant tunneling through a corresponding quantized level in the dot. Resonant tunneling of the Nth electron occurs when the total energy before and after the tunneling is conserved. The resonance spacing between coulomb-blockade peaks is given by

$$\Delta_2 \equiv \Delta\epsilon_F \;=\; (E_{N+1} - E_N) + e^2/C$$

The charging energy is much larger than the mean level spacing in the dot so that the coulomb-blockade peaks are almost equidistant. The tunneling is suppressed between resonances primarily by the charging energy.

V. CONDUCTANCE FLUCTUATIONS IN ALMOST CLOSED QUANTUM DOTS

The objective of this paper is to derive an analytical formulation of the mesoscopic conductance fluctuations of almost closed quantum dots at low temperature. We consider the dots of arbitrary shape, with or without disorder and electron-electron (e-e) interactions. Based on the dot-shape, the electron dynamics in the absence of disorder can be chaotic, integrable or non-integrable (intermediate between the two regimes) and the randomness arises due to scattering from the boundaries. For chaotic shape and/or weak disorder, the quantum dynamics is delocalized and the energy levels and eigenfunctions of the dot-Hamiltonian exhibit universal statistical fluctuations that can be well-modeled by the Wigner-Dyson random ensembles. However, at low temperatures and in coulomb-blockade regime, the dot properties e.g. transport display mesoscopic fluctuations as a function of the system conditions e.g. gate voltage, shape, disorder etc. The origin of these system-dependent fluctuations seems linked to the dominance of particle-interactions at low temperatures. The theoretical treatment in this regime therefore requires a more generalized, that is, system-dependent random matrix approach. A similar need arises from the analysis of the dots of non-integrable shape and/or strong disorder where inhomogeneous scattering may lead to partial localized electron-waves. For such dots, the Wigner-Dyson model is not expected to be applicable even in absence of the e-e interactions.

For this analysis the quantum coulomb-blockade region is considered, where the temperature is comparable to or smaller than the mean level spacing in the dot. The e-e interactions in this model are taken into account by introducing the correlations among the matrix elements. I model the dot-statistics by an ensemble of the spinless interacting fermions:

$$H = \sum_{ij} V_{ij} a_i^+ a_j + \frac{1}{4} \sum_{ijkl} U^A_{ijkl} a_i^+ a_j^+ a_l a_k \qquad (6)$$

here the states $|i> = a_i^+|0>$ describe a fixed basis of m single-particle states with V_{ij} as the matrix elements of the one body Hamiltonian and U_{ijkl} as the antisymmetrized matrix elements of the two body interaction U.

A specific ensemble of Hamiltonians, referred as random interaction matrix model (RIMM)[26], was introduced to study generic fluctuations in chaotic dots with interactions. The RIMM considers both one body matrix elements V_{kl} and the antisymmetrized two body matrix elements $U^A_{ij;kl} = U_{ij;kl} - U_{ij;lk}$ (in 2-particle space) chosen from Wigner-Dyson ensembles and is therefore applicable only for the chaotic or weakly disordered dots with homogeneous interactions. To model the cases with mixed dynamics or non-homogeneous interactions inside the dot, a generalization of RIMM is desirable. For this purpose, I model H in Eq.(6) by an ensemble of Hermitian matrices with multiparametric, correlated, Gaussian distributed matrix elements.

A. System with time reversal symmetry

The joint probability P_{N1} of the components ψ_{nk}, $n = 1 \to N$, of an eigenvector ψ_k of the Hamiltonian H (Eq.(6)) can be defined as follows,

$$P_{N1}(Z_{1k}, Z_{2k}..., Z_{Nk}; Y) \;=\; \int \tilde{f}_k \, \rho(H, Y) \, \mathrm{d}H \quad (7)$$

with $\tilde{f}_k = \prod_{m=1}^{N} \delta(Z_{mk} - \psi_{mk}) \delta^{\beta-1}(Z^*_{mk} - \psi^*_{mk})$ and $\beta = 1$. Here Y is the complexity parameter. The Y-govrened diffusion equation of the wave-function is given by[27]

$$\frac{\partial P_{N1}}{\partial Y} \;=\; \frac{2}{4D^2} \sum_{n=1}^{N} \frac{\partial}{\partial Z_{nk}} \left(h_1 + \sum_{m=1}^{N} \frac{\partial h_2}{\partial Z_{mk}} \right) \quad (8)$$

with $h_1 = (N-1)\chi Z_{nk} P_{N1}$, $h_2 = \chi(\delta_{mn} - Z_{nk} Z_{mk}) P_{N1}$. D is the local mean level spacing at a given energy and χ is related to the average localization length of the eigenfunction Z_k.

1. Partial-width amplitude distribution

The joint distribution of the partial-width amplitudes $\gamma = (\gamma_1, \gamma_2, \gamma_3, \ldots \gamma_N)$ of a resonance k is given by

$$P_\gamma \;=\; C \int \prod_{j=1}^{N} \delta(\gamma_j - X_j) P_{N1} \, \mathrm{d}Z \qquad (9)$$

where P_{N1} is the joint distribution of the components $Z_{jk}, j = 1 \to N$ of an eigenfunction say Z_k as a function of complexity parameter Y[27], $dZ \equiv \prod_{j=1}^{N} dZ_{jk}$, C is the normalization constant. $X_j = \sum_l \phi^*_{lj} Z_{lk}$ is the partial-width amplitude of resonance (scalar product of the channel wavefunction ϕ_{lj} and the resonance wavefunction Z_{lk}). With help of Eq.(8), the diffusion equation for P_γ can now be obtained

$$\frac{\partial P_\gamma}{\partial Y} = C_0 \left(I_1 + I_2 + I_3\right) \tag{10}$$

where $C_0 = 2\chi C/4D^2$ and

$$\begin{aligned} I_1 &= (N-1) \int f \sum_{n=1}^{N} \frac{\partial (Z_{nk} P_{N1})}{\partial Z_{nk}} \, \mathrm{d}Z \\ I_2 &= \int f \sum_{n=1}^{N} \frac{\partial^2 P_{N1}}{\partial Z_{nk}^2} \, \mathrm{d}Z \\ I_3 &= -\int f \sum_{n,m=1}^{N} \frac{\partial^2 (Z_{nk} Z_{mk} P_{N1})}{\partial Z_{nk} \partial Z_{mk}} \, \mathrm{d}Z \end{aligned}$$

with $f = \prod_{j=1}^{N} \delta(\gamma_j - X_j)$ The next step is to rewrite the integrals in Eqs.(10) in terms of the γ-derivatives. Using partial integration, the term I_1 can further be reduced,

$$I_1 = -(N-1) \sum_n \int \frac{\partial f}{\partial Z_{nk}} \left(Z_{nk} P_{N1}\right) \mathrm{d}Z$$

Now as $X_p = \sum_l \phi^*_{lp} Z_{lk}$, this gives $\frac{\partial X_p}{\partial Z_{nk}} = \phi^*_{np}$ which further gives

$$\begin{aligned} \frac{\partial f}{\partial Z_{nk}} &= -\sum_{p=1}^{N} \frac{\partial f}{\partial \gamma_p} \frac{\partial X_p}{\partial Z_{nk}} \\ &= -\sum_{p=1}^{N} \frac{\partial f}{\partial \gamma_p} \phi^*_{np} \end{aligned}$$

Substitution of the above equation in I_1 gives

$$\begin{aligned} I_1 &= (N-1) \sum_n \sum_p \frac{\partial}{\partial \gamma_p} \int f \, \phi^*_{np} \left(Z_{nk} P_{N1}\right) \mathrm{d}Z \\ &= (N-1) \sum_p \frac{\partial}{\partial \gamma_p} \int f \left(\sum_n \phi^*_{np} Z_{nk}\right) P_{N1} \, \mathrm{d}Z \\ &= \frac{1}{C} (N-1) \sum_p \frac{\partial}{\partial \gamma_p} \left(\gamma_p \, P_\gamma\right) \end{aligned} \tag{11}$$

Similarly a repeated use of the partial integration and the relations $\frac{\partial^2 X_p}{\partial Z_{nk}^2} = 0$ reduces I_2 in Eq.(10):

$$\begin{aligned} I_2 &= -\sum_n \int \frac{\partial f}{\partial Z_{nk}} \frac{\partial P_{N1}}{\partial Z_{nk}} \, \mathrm{d}Z \\ &= \sum_p \frac{\partial}{\partial \gamma_p} \sum_s \frac{\partial}{\partial \gamma_s} \int f \left(\sum_n \phi^*_{np} \phi^*_{ns}\right) P_{N1} \, \mathrm{d}Z \end{aligned}$$

For system with time-reversal symmetry $\phi^*_{np} = \phi_{np}$. The orthogonality of the channel wavefunctions i.e $\sum_n \phi^*_{np} \phi^*_{ns} = \delta_{sp}$ leads to further simplification:

$$\begin{aligned} I_2 &= \frac{1}{C} \sum_p \frac{\partial}{\partial \gamma_p} \sum_s \frac{\partial}{\partial \gamma_s} \left(\delta_{sp} P_\gamma\right) \\ &= \frac{1}{C} \sum_p \frac{\partial^2 P_\gamma}{\partial \gamma_p^2} \end{aligned} \tag{12}$$

Similarly I_3 in Eq.(10) can be expressed as a 2nd order derivative,

$$\begin{aligned} I_3 &= \sum_{nm} \int \frac{\partial f}{\partial Z_{nk}} \frac{\partial}{\partial Z_{mk}} \left(Z_{nk} Z_{mk} P_{N1}\right) \, \mathrm{d}Z \\ &= -\frac{1}{C} \sum_{ps} \frac{\partial^2}{\partial \gamma_p \partial \gamma_s} \left(\gamma_p \, \gamma_s \, P_\gamma\right) \end{aligned} \tag{13}$$

Substitution of I_1, I_2, I_3 from Eqs.(11, 12, 13) in Eq.(10) leads to the diffusion equation of partial-width amplitude

$$\begin{aligned} \frac{\partial P_\gamma}{\partial Y} &= (N-1) \sum_p \frac{\partial}{\partial \gamma_p} \left(\gamma_p \, P_\gamma\right) - \sum_{ps} \frac{\partial^2}{\partial \gamma_p \partial \gamma_s} \left(\gamma_p \, \gamma_s \, P_\gamma\right) \\ &+ \sum_p \frac{\partial^2 P_\gamma}{\partial \gamma_p^2} \end{aligned} \tag{14}$$

As $Y \to \infty$, P_γ reaches a steady state which corresponds to a Gaussian distribution

$$P_\gamma(\gamma) = (detM)^{-\beta/2} \mathrm{e}^{-(\beta/2)\gamma^\dagger \, M^{-1}\gamma} \tag{15}$$

with M as the $N \times N$ channel correlation matrix: $M_{cc'} = \overline{\gamma^*_c \gamma'_c} = N^{-1} \langle \phi_c | \phi'_c \rangle$. The same result is obtained if one consider the distribution P_{N1} given by the eigenfunctions of a Wigner-Dyson ensemble[5]. This is expected because the solution of Eq.(10) in limit $Y \to \infty$ limit is indeed a Wigner-Dyson ensemble.

2. Width distribution

Here we consider a symmetric dot $\Gamma^l = \Gamma^r$. The resonance width Γ is a function of the partial width amplitudes,

$$\Gamma = \sum_{j=1}^{N} \gamma^*_j \gamma_j \tag{16}$$

where $\gamma^*_j = \gamma_j$. The peak width-distribution can then be given as

$$P_\tau(\Gamma) = \int \delta(\Gamma - \sum_{j=1}^{N} \gamma^*_j \gamma_j) \, P_\gamma(\gamma_1 \, , \gamma_2 \, . . \gamma_N) \, \mathrm{d}\gamma \tag{17}$$

As discussed in[28], the Wigner-Dyson limit of P_τ depends on the channel correlation matrix M. For the case of uncorrelated and equivalent channels, M has all degenerate

eigenvalues which results in a χ^2_ν distribution of P_τ (with $\nu = \beta N$ as the degrees of freedom, $\beta = 1$ in this case)[23]:

$$P_\tau(\Gamma) \propto \Gamma^{\nu/2-1} \exp\left[-\nu\Gamma/2\overline{\Gamma}\right]$$

For the multiparametric Gaussian ensemble case, We therefore proceed by a route different from the one used in[28] and derive the Y-based formulation of P_τ.

Differentiating Eq.(17) with respect to Y gives

$$\frac{\partial P_\tau(\Gamma)}{\partial Y} = \int h \, \frac{\partial P_\gamma}{\partial Y} \, \mathrm{d}\gamma \tag{18}$$

where $h = \delta(\Gamma - \sum_j \gamma_j^* \gamma_j)$. We derive the Y governed evolution of $P_\tau(\Gamma)$ as follows:

$$\frac{\partial P_\tau(\Gamma)}{\partial Y} = \frac{2\chi}{4D^2}\left(J_1 + J_2 + J_3\right) \tag{19}$$

where

$$\begin{aligned} J_1 &= (N-1)\int h \, \left[\sum_p \frac{\partial}{\partial \gamma_p}(\gamma_p P_\gamma)\right] \, \mathrm{d}\gamma \\ J_2 &= \int h \, \left[\sum_p \frac{\partial^2 P_\gamma}{\partial \gamma_p^2}\right] \, \mathrm{d}\gamma \\ J_3 &= -\int h \, \left[\sum_{ps} \frac{\partial^2}{\partial \gamma_p \partial \gamma_s}(\gamma_p \, \gamma_s \, P_\gamma)\right] \, \mathrm{d}\gamma \end{aligned}$$

Using the partial integration and vanishing of P_γ at the end-points, J_1 can be rewritten as

$$J_1 = -(N-1)\int \sum_p \int \frac{\partial h}{\partial \gamma_p}\left(\gamma_p P_\gamma\right) \, \mathrm{d}\gamma$$

Now as $\frac{\partial h}{\partial \gamma_p} = -\sum_{t=1}^{N} \frac{\partial h}{\partial \Gamma} \, \frac{\partial}{\partial \gamma_p}(\gamma_t^* \gamma_t)$ and $\sum_t \frac{\partial}{\partial \gamma_p}(\gamma_t^* \gamma_t) = \sum_t \frac{\partial}{\partial \gamma_p}(\gamma_t^2) = 2\sum_t \gamma_t \frac{\partial \gamma_t}{\partial \gamma_p} = 2\sum_t \gamma_t \delta_{tp} = 2\gamma_p$

J_1 can further be reduced

$$\begin{aligned} J_1 &= -(N-1)\sum_p \int \frac{\partial h}{\partial \gamma_p}\left(\gamma_p P_\gamma\right) \, \mathrm{d}\gamma \\ &= (N-1)\sum_p \sum_t \frac{\partial}{\partial \Gamma}\int h \, \frac{\partial}{\partial \gamma_p}(\gamma_t^* \gamma_t)\left(\gamma_p P_\gamma\right) \, \mathrm{d}\gamma \\ &= (N-1)\sum_p \frac{\partial}{\partial \Gamma}\int h \, (2\gamma_p) \, \gamma_p P_\gamma \, \mathrm{d}\gamma \\ &= 2(N-1)\frac{\partial}{\partial \Gamma}\left(\sum_p \gamma_p^2 \, P_\Gamma\right) \\ &= 2(N-1)\frac{\partial}{\partial \Gamma}\left(\Gamma \, P_\Gamma\right) \end{aligned} \tag{20}$$

The second order derivative in J_2 can be removed by repeated partial integrations. Using the relation $\sum_t \frac{\partial^2}{\partial \gamma_p^2}(\gamma_t^2) = \sum_t \frac{\partial}{\partial \gamma_p}(2\gamma_t \delta_{tp}) = 2\sum_t \delta_{tp}$ and $\sum_w \frac{\partial}{\partial \gamma_p}(\gamma_w^2) = 2\sum_w \gamma_w \frac{\partial \gamma_w}{\partial \gamma_p} = 2\sum_w \gamma_w \delta_{wp} = 2\gamma_p$, it can further be reduced

$$\begin{aligned} J_2 &= -\sum_p \int \frac{\partial h}{\partial \gamma_p} \, \frac{\partial P_\gamma}{\partial \gamma_p} \, \mathrm{d}\gamma \\ &= \sum_p \frac{\partial^2}{\partial \Gamma^2}\int h \, (2\gamma_p) \, (2\gamma_p) P_\gamma \, \mathrm{d}\gamma \\ &- 2\sum_p \frac{\partial}{\partial \Gamma}\int h \, \sum_t \delta_{tp} P_\gamma \, \mathrm{d}\gamma \\ &= 4\frac{\partial^2}{\partial \Gamma^2}\left(\Gamma \, P_\Gamma\right) - 2N\frac{\partial P_\Gamma}{\partial \Gamma} \end{aligned} \tag{21}$$

Following similar steps as above, J_3 can also be reduced as a function of Γ,

$$\begin{aligned} J_3 &= \sum_{ps} \int \frac{\partial h}{\partial \gamma_p}\frac{\partial}{\partial \gamma_s}\left(\gamma_p \, \gamma_s \, P_\gamma\right) \, \mathrm{d}\gamma \\ &= -4\sum_{ps} \frac{\partial^2}{\partial \Gamma^2}\left(\gamma_p^2 \, \gamma_s^2 P_\Gamma\right) + 2\sum_{ps} \frac{\partial}{\partial \Gamma}\left(\delta_{ps} \, \gamma_p \, \gamma_s \, P_\Gamma\right) \\ &= -4\frac{\partial^2}{\partial \Gamma^2}\left(\Gamma^2 \, P_\Gamma\right) + 2\frac{\partial}{\partial \Gamma}\left(\Gamma \, P_\Gamma\right) \end{aligned} \tag{22}$$

Sustituting J_1, J_2, J_3 from Eqs.(20, 21, 22) in Eq.(19), we get the width-distribution

$$\frac{\partial P_\tau(\Gamma)}{\partial Y} = B_0 \frac{\partial}{\partial \Gamma}\left[(f_1(\Gamma))P_\Gamma + 2\frac{\partial}{\partial \Gamma}(f_2(\Gamma))P_\Gamma\right] \tag{23}$$

where $B_0 = \frac{\chi}{D^2}$, D is the local mean level spacing at a given energy, χ is related to localization length of the eigenvector, $f_1(\Gamma) = N(\Gamma - 1)$, $f_2(\Gamma) = (1-\Gamma)\Gamma$.

Eq.(23) can now be used to derive the single-parametric formulation of the conductance peak-height distribution.

3. Peak-height distribution

In a almost-closed dot, the conductance at resonance is $g = \frac{e^2 \pi \Gamma}{h 4kT} = c \, \Gamma$. The conductance peak height is measured in units of $\frac{e^2}{h}\frac{\pi\Gamma}{4kT}$. The joint-distribution of peak-height can be computed from the width distribution $P_\tau(\Gamma)$.

$$P_g(g) = \int \delta(g - c\Gamma) \, P_\tau(\Gamma) \, \mathrm{d}\Gamma \tag{24}$$

This implies

$$\frac{\partial P_g(g)}{\partial Y} = \int \delta(g - c\Gamma) \, \frac{\partial P_\tau(\Gamma)}{\partial Y} \, \mathrm{d}\Gamma \tag{25}$$

Substituing Eq.(23) in eq.(25), the Y-evolution of P_γ can be obtained

$$\frac{\partial P_g(g)}{\partial Y} = B_0 N \int u \, \frac{\partial}{\partial \Gamma}(\Gamma - 1) \, P_\tau \, \mathrm{d}\Gamma + 2B_0 \int u \, \frac{\partial^2}{\partial \Gamma^2}(1-\Gamma)\Gamma \, P_\tau \, \mathrm{d}\Gamma \quad (26)$$

with $u \equiv \delta(g - c\Gamma)$.

Proceeding as in the case of P_τ distribution, the integrals in the above equation can be evaluated. This leads to following Y governed evolution of P_g,

$$\frac{\partial P_g(g)}{\partial Y} = B_0 \left[\frac{\partial}{\partial g}(f_1(g)) P_g + 2 \frac{\partial^2}{\partial g^2}(f_2(g)) P_g \right] \quad (27)$$

where $f_1(g) = N(g-c), f_2(g) = (c-g)g, c = \frac{e^2}{h}\frac{\pi}{4kT}$

B. System with no time reversal symmetry

The joint probability distribution P_{N1} for the wavefunction components in this case can be defined by Eq.(7) with $\beta = 2$. The evolution equation for Y-governed diffusion of P_{N1} is[27]

$$\frac{\partial P_{N1}}{\partial Y} = \frac{2}{4D^2} \sum_{n=1}^{N} \frac{\partial}{\partial Z_{nk}} \left(h_1 + \sum_{m=1}^{N} \frac{\partial h_2}{\partial Z^*_{mk}} \right) \quad (28)$$

with $h_1 = (N-1)\chi Z_{nk} P_{N1}$, $h_2 = \chi(\delta_{mn} - Z_{nk} Z^*_{mk}) P_{N1}$. D is the local mean level spacing at a given energy and χ is related to the average localization length of the eigenfunction Z_k.

1. Partial-width amplitude distribution

The joint distribution of the partial-width amplitudes $\gamma = (\gamma_1, \gamma_2, \gamma_3, \ldots \gamma_N)$ of a resonance k is given by

$$P_\gamma = C \int \prod_{j=1}^{N} \delta^2(\gamma_j - X_j) \, P_{N1} \mathrm{d}Z \quad (29)$$

where P_{N1} is the joint distribution of the components $Z_{jk}, j = 1 \to N$ of an eigenfunction say Z_k as a function of complexity parameter Y[27], $dZ \equiv \prod_{j=1}^{N} dZ^*_{jk} dZ_{jk}$, C is the normalization constant. $X_j = \sum_l \phi^*_{lj} Z_{lk}$ is the partial-width amplitude of resonance (scalar product of channel wavefunction ϕ_j and resonance wavefunction Z_k). With help of Eq.(28), the diffusion equation for P_γ can now be obtained:

$$\frac{\partial P_\gamma}{\partial Y} = C_0 \left(I_1 + I_2 + I_3 \right) \quad (30)$$

where $C_0 = 2\chi C / 4D^2$ and

$$I_1 = (N-1) \int f \sum_{n=1}^{N} \frac{\partial (Z_{nk} P_{N1})}{\partial Z_{nk}} dZ$$

$$I_2 = \int f \sum_{n=1}^{N} \frac{\partial^2 P_{N1}}{\partial Z_{nk} \partial Z^*_{nk}} \, dZ$$

$$I_3 = -\int f \sum_{n,m=1}^{N} \frac{\partial^2 (Z_{nk} Z^*_{mk} P_{N1})}{\partial Z_{nk} \partial Z^*_{mk}} \, \mathrm{d}Z$$

with $f = \prod_{j=1}^{N} \delta^2(\gamma_j - X_j)$.

The next step is to rewrite the integrals in Eqs.(30) in terms of the γ-derivatives. Using partial integration, the term I_1 can further be reduced,

$$I_1 = -(N-1) \sum_n \int \frac{\partial f}{\partial Z_{nk}} \, (Z_{nk} P_{N1}) \, \mathrm{d}Z$$

Now as $X_p = \sum_l \phi^*_{lp} Z_{lk}$ and $X^*_q = \sum_l \phi_{lq} Z^*_{lk}$, this gives $\frac{\partial X_p}{\partial Z_{nk}} = \phi^*_{np}$ and $\frac{\partial X^*_q}{\partial Z_{nk}} = 0$ which further gives

$$\frac{\partial f}{\partial Z_{nk}} = -\sum_{p=1}^{N} \frac{\partial f}{\partial \gamma_p} \frac{\partial X_p}{\partial Z_{nk}} - \sum_{q=1}^{N} \frac{\partial f}{\partial \gamma^*_q} \frac{\partial X^*_q}{\partial Z_{nk}} = -\sum_{p=1}^{N} \frac{\partial f}{\partial \gamma_p} \, \phi^*_{np}$$

Substitution of the above equation in I_1 gives

$$I_1 = (N-1) \sum_n \sum_p \frac{\partial}{\partial \gamma_p} \int f \, \phi^*_{np} \, (Z_{nk} P_{N1}) \, \mathrm{d}Z = (N-1) \sum_p \frac{\partial}{\partial \gamma_p} \int f \, \left(\sum_n \phi^*_{np} Z_{nk} \right) \, P_{N1} \, \mathrm{d}Z = \frac{1}{C}(N-1) \sum_p \frac{\partial}{\partial \gamma_p} (\gamma_p \, P_\gamma) \quad (31)$$

Similarly a repeated use of the partial integration and the relations $\frac{\partial^2 X_p}{\partial Z^*_{nk} \partial Z_{nk}} = 0$ reduces I_2 in Eq.(30)

$$I_2 = -\sum_n \int \frac{\partial f}{\partial Z_{nk}} \frac{\partial P_{N1}}{\partial Z^*_{nk}} \, \mathrm{d}Z = \sum_p \frac{\partial}{\partial \gamma_p} \sum_v \frac{\partial}{\partial \gamma^*_v} \int f \left(\sum_n \phi_{nv} \, \phi^*_{np} \right) \, P_{N1} \, \mathrm{d}Z$$

The orthogonality of the channel wavefunctions i.e $\sum_n \phi_{nv} \, \phi^*_{np} = \delta_{vp}$ leads to further simplification:

$$I_2 = \frac{1}{C} \sum_p \frac{\partial}{\partial \gamma_p} \sum_v \frac{\partial}{\partial \gamma^*_v} (\delta_{vp} P_\gamma) = \frac{1}{C} \sum_p \frac{\partial^2 P_\gamma}{\partial \gamma_p \partial \gamma^*_p} \quad (32)$$

Similarly I_3 in Eq.(30) can be expressed as a 2nd order derivative,

$$\begin{aligned} I_3 &= \sum_{n,m} \int \frac{\partial f}{\partial Z_{nk}} \frac{\partial}{\partial Z^*_{mk}} (Z_{nk} Z^*_{mk} P_{N1}) \ \mathrm{d}Z \\ &= -\frac{1}{C} \sum_{ps} \frac{\partial^2}{\partial \gamma_p \partial \gamma^*_s} (\gamma_p \ \gamma^*_s \ P_\gamma) \end{aligned} \tag{33}$$

Substitution of I_1, I_2, I_3 from Eqs.(31, 32, 33) in Eq.(30) leads to the diffusion equation of partial-width amplitude

$$\begin{aligned} \frac{C}{C_0} \frac{\partial P_\gamma}{\partial Y} &= (N-1) \sum_p \frac{\partial}{\partial \gamma_p} (\gamma_p \ P_\gamma) + \sum_p \frac{\partial^2 P_\gamma}{\partial \gamma_p \partial \gamma^*_p} \\ &- \sum_{p,s} \frac{\partial^2}{\partial \gamma_p \partial \gamma^*_s} (\gamma_p \ \gamma^*_s \ P_\gamma) \end{aligned} \tag{34}$$

In this case, the limit $Y \to \infty$ again leads to steady state. The steady state distribution is given by Eq.(15) however for $\beta = 2$.

2. Width distribution

Here we consider a symmetric dot $\Gamma^l = \Gamma^r$. The resonace width Γ is a function of the partial width amplitudes,

$$\Gamma = \sum_{j=1}^{N} \gamma^*_j \gamma_j \tag{35}$$

The peak width-distribution can then be given as

$$P_\tau(\Gamma) = \int \delta(\Gamma - \sum_{j=1}^{N} \gamma^*_j \gamma_j) \ P_\gamma(\gamma_1 \ , \gamma_2 \ . . \gamma_N) \ \mathrm{d}\gamma \tag{36}$$

The χ^2_ν distribution for system without time-reversal symmetry case of $P_\tau(\Gamma)$ (with $\nu = \beta N$ as the degrees of freedom,$\beta = 2$ for this case) is given by Eq.(18).

Differentiating Eq.(36) with respect to Y gives

$$\frac{\partial P_\tau(\Gamma)}{\partial Y} = \int h \ \frac{\partial P_\gamma}{\partial Y} \ \mathrm{d}\gamma \tag{37}$$

where $h = \delta(\Gamma - \sum_j \gamma^*_j \gamma_j)$. Eq.(34) can then be used to derive the Y governed evolution of $P_\tau(\Gamma)$ as follows:

$$\frac{\partial P_\tau(\Gamma)}{\partial Y} = \frac{2\chi}{4D^2} (J_1 + J_2 + J_3) \tag{38}$$

where

$$\begin{aligned} J_1 &= (N-1) \int h \ \left[\sum_p \frac{\partial}{\partial \gamma_p} (\gamma_p P_\gamma) \right] \ \mathrm{d}\gamma \\ J_2 &= \int h \ \left[\sum_p \frac{\partial^2 P_\gamma}{\partial \gamma_p \partial \gamma^*_p} \right] \ \mathrm{d}\gamma \\ J_3 &= -\int h \ \left[\sum_{ps} \frac{\partial^2}{\partial \gamma_p \partial \gamma^*_s} (\gamma_p \ \gamma^*_s \ P_\gamma) \right] \ \mathrm{d}\gamma \end{aligned}$$

Using the partial integration and vanishing of P_γ at the end-points, J_1 can be rewritten as

$$J_1 = -(N-1) \sum_p \int \frac{\partial h}{\partial \gamma_p} (\gamma_p P_\gamma) \ \mathrm{d}\gamma$$

Now as $\frac{\partial h}{\partial \gamma_p} = -\sum_{t=1}^{N} \frac{\partial h}{\partial \Gamma} \ \frac{\partial}{\partial \gamma_p} (\gamma^*_t \gamma_t)$ and $\frac{\partial}{\partial \gamma_p} (\gamma^*_t \gamma_t) = \sum_t (\gamma^*_t \delta_{tp}) = \gamma^*_p$
J_1 can further be reduced

$$\begin{aligned} J_1 &= (N-1) \sum_p \sum_t \frac{\partial}{\partial \Gamma} \int h \ \frac{\partial}{\partial \gamma_p} (\gamma^*_t \gamma_t) (\gamma_p P_\gamma) \ \mathrm{d}\gamma \\ &= (N-1) \sum_p \frac{\partial}{\partial \Gamma} \int h \ \gamma^*_p \ \gamma_p \ P_\gamma \ \mathrm{d}\gamma \\ &= (N-1) \frac{\partial}{\partial \Gamma} \int h \left(\sum_p \gamma^*_p \ \gamma_p \right) \ P_\gamma \ \mathrm{d}\gamma \\ &= (N-1) \frac{\partial}{\partial \Gamma} (\Gamma \ P_\Gamma) \end{aligned} \tag{39}$$

The second order derivative in J_2 can be removed by repeated partial integrations. Using the relation $\sum_p \sum_t \frac{\partial^2}{\partial \gamma^*_p \partial \gamma_p} (\gamma^*_t \gamma_t) = \sum_p \sum_t \frac{\partial}{\partial \gamma^*_p} (\gamma^*_t \delta_{tp}) = \sum_{pt} \delta_{tp}$, it can further be reduced

$$\begin{aligned} J_2 &= -\sum_p \int \frac{\partial h}{\partial \gamma_p} \ \frac{\partial P_\gamma}{\partial \gamma_{p^*}} \ \mathrm{d}\gamma \\ &= \frac{\partial^2}{\partial \Gamma^2} \left[(\sum_p \gamma^*_p \gamma_p) P_\Gamma \right] - \frac{\partial}{\partial \Gamma} \left(\sum_{pt} \delta_{pt} \ P_\Gamma \right) \\ &= \frac{\partial^2}{\partial \Gamma^2} (\Gamma \ P_\Gamma) - N \frac{\partial P_\Gamma}{\partial \Gamma} \end{aligned} \tag{40}$$

Following similar steps as above, J_3 can also be reduced as a function of Γ,

$$\begin{aligned} J_3 &= \sum_{ps} \int \frac{\partial h}{\partial \gamma_p} \ \frac{\partial}{\partial \gamma^*_s} (\gamma_p \ \gamma^*_s \ P_\gamma) \ \mathrm{d}\gamma \\ &= -\sum_{ps} \frac{\partial^2}{\partial \Gamma^2} \int h \ \gamma_s \gamma^*_p \gamma_p \gamma^*_s \ P_\gamma \ \mathrm{d}\gamma \\ &+ \sum_{ps} \frac{\partial}{\partial \Gamma} \int h \ \delta_{ps} \ \gamma_p \gamma^*_s \ P_\gamma \ \mathrm{d}\gamma \\ &= -\frac{\partial^2}{\partial \Gamma^2} \left(\Gamma^2 \ P_\Gamma \right) + \frac{\partial}{\partial \Gamma} (\Gamma \ P_\Gamma) \end{aligned} \tag{41}$$

Sustituting J_1, J_2, J_3 from Eqs.(39, 40, 41) in Eq.(38), we get the width-distribution

$$\frac{\partial P_\tau(\Gamma)}{\partial Y} = B_1 \frac{\partial}{\partial \Gamma} \left[(f_1(\Gamma)) P_\Gamma + \frac{\partial}{\partial \Gamma} (f_2(\Gamma)) P_\Gamma \right] \tag{42}$$

where $B_1 = \frac{2\chi}{4D^2}$, D is the local mean level spacing at a given energy, χ is related to localization length of the eigenvector, $f_1(\Gamma) = N(\Gamma - 1), f_2(\Gamma) = (1 - \Gamma)\Gamma$

Eq.(42) can now be used to derive the single-parametric formulation of the conductance peak-height distribution.

3. Peak-height distribution

In a almost-closed dot, the conductance at resonance is $g = \frac{e^2 \pi \Gamma}{h 4kT} = c\ \Gamma$. The conductance peak height is measured in units of $\frac{e^2}{h}\frac{\pi\Gamma}{4kT}$. The joint-distribution of peak-height can be computed from the width distribution $P_\tau(\Gamma)$.

$$P_g(g) \ = \ \int \delta(g - c\Gamma)\ P_\tau(\Gamma)\ \mathrm{d}\Gamma \tag{43}$$

This implies

$$\frac{\partial P_g(g)}{\partial Y} \ = \ \int \delta(g - c\Gamma)\ \frac{\partial P_\tau}{\partial Y}\ \mathrm{d}\Gamma \tag{44}$$

Substituing eq.(42) in eq.(44), the Y-evolution of P_γ can be obtained

$$\begin{aligned}\frac{\partial P_g(g)}{\partial Y} \ &= \ B_1 N \int u\ \frac{\partial}{\partial \Gamma}(\Gamma - 1)\ P_\Gamma\ \mathrm{d}\Gamma \\ &+ \ B_1 \int u\ \frac{\partial^2}{\partial \Gamma^2}\left[(1-\Gamma)\Gamma\ P_\Gamma\right)\ \mathrm{d}\Gamma\end{aligned} \tag{45}$$

with $u \equiv \delta(g - c\Gamma)$. Proceeding as in the case of P_Γ distribution, the integrals in the above equation can be evaluated. This leads to following Y governed evolution of P_g,

$$\frac{\partial P_g(g)}{\partial Y} = B_1 \left[\frac{\partial}{\partial g}(f_1(g))P_g + \frac{\partial^2}{\partial g^2}(f_2(g))P_g\right] \tag{46}$$

where $f_1(g) = N(g - c)$, $f_2(g) = (c - g)g$, $c = \frac{e^2}{h}\frac{\pi}{4kT}$

VI. CONCLUSION

The complexity parameter formulation of the eigenvalues or eigenfunctions statistics suggests that the sample to sample fluctuations of conductance is not sensitive to the origin of the interactions, random or non-random. It is influenced only by the degree of uncertainty associated with the formulation. The system dependence in $P_g(g)$ enters only through Y and the system size N. This suggests the possibility of various universality classes of conductance fluctuations defined by the complexity parameter. Quantum dots have become a powerful tool for investigating the physical properties of small coherent quantum systems. The ability to control their shape, size and the number of electrons has made them practically useful for experimental studies. The formulation can further be used to analyze the critical behavior of nanosystems. The study of quantum dots are considered to have a wide field of application in quantum information technology e.g. Quantum Computer.

[1] Van Kampen, N.G., 1981, Stochastic Process in Physics and Chemistry (North Holland, Amsterdam).

[2] U. Meirav, M. A. Kanster and S. J. Wind, 1990, Single-Electron Charging and Periodic Conductance Resonances in GaAs Nanostructures, Phys. Rev. Lett.65, 771.

[3] P. L. McEuen., N. S. Wingreen, E. B. Foxman, J. Kinaret, U. Meirav, M. A. Kastner and Y. Meir, 1993, Coulomb Interactions and Energy-Level Spectrum of a Small Electron Gas, Physica B 189, 70.

[4] Akkermans, E. G. Montambaux, J. L. Pichard and J. Zinn-Justin, 1995, Mesoscopic Quantum Physics (North-Holland, Amsterdam).

[5] Y. Alhassid, 2000, Statistical Theory of Quantum Dots, Reviews of Modern Physics 72, 895.

[6] Ralph, D.C., C.T. Black, and M. Tinkham, 1997, Gate-voltage Studies of Discrete Electronic States in Aluminum Nanoparticles, Phys. Rev. Lett., 78, 4087.

[7] Davidovic, D., and M. Tinkham, 1999, Spectroscopy, Interactions and Level splitting in Au Nanoparticles, Phys. Rev. Lett. 83, 1644.

[8] Porath, D., and O. Millo, 1996, Single Electron Tunneling and Level Spectroscopy of Isolated C60 Molecules, J. Appl. Phys. 81, 2241.

[9] Bockrath, M., D.H. Cobden, P.L. Mceuen, N.G. Chopra, A. Zettl, A. Thess and R.E. Smalley, 1997, Single-Electron Transport in Ropes of Carbon Nanotubes, Science 275, 1922.

[10] U. Meirav, M. A. Kanster and S. J. Wind, 1990, Single-Electron Charging and Periodic Conductance Resonances in GaAs Nanostructures, Phys. Rev. Lett.65, 771.

[11] P. L. McEuen., N. S. Wingreen, E. B. Foxman, J. Kinaret, U. Meirav, M. A. Kastner and Y. Meir, 1993, Coulomb Interactions and Energy-Level Spectrum of a Small Electron Gas, Physica B 189, 70.

[12] M. A. Kastner, 1992, The Single-Electron Transistor, Rev. Mod. Phys. 64, 849.

[13] M. A. Kastner, 1993, Artificial Atoms, Phys. Today 46 (1), 24.

[14] Ashoori, R.C., 1996, Electrons in Artificial Atoms, Nature (London) 379, 413.

[15] Cobden D. H., M. Bockrath, P. L. McEuen, A. G. Rinzler, and R. E. Smalley, 1998, Spin Splitting and Even-Odd Effects in Carbon Nanotubes, Phys. Rev. Lett. 81, 681.

[16] Altshuler, B. L., 1985, Fluctuations in the Extrinsic Conductivity of Disordered Conductors, JETP Lett. 41, 648.

[17] Lee. P. A. and A. D. Stone, 1985, Universal Conductance Fluctuations in Metals, Phys. Rev. Lett. 55, 1622.

[18] Tarucha, S., D. G. Austing, T. Honda, R. J. van dr hage, and L. P. Kouwenhoven, 1996, Shell Filling and Spin Effects in a Few Electron Quantum Dot, Phys. Rev. Lett. 77, 3613.

[19] Giaever, I., and H. R. Zeller, 1968, Superconductivity of

Small Tin Particles Measured by Tunneling, Phys. Rev. Lett. 20, 1504.
[20] Altshuler, B. L., and B. I. Shklovskii, 1986, Sov. Phys. JETP 64, 127.
[21] Imry, Y., 1986a, Europhys. Lett. 1249.
[22] Edwards, J.T., and D. J. Thouless, 1972, Numerical Studies of Localization in Disordered Systems, J. Phys. C 5, 807.
[23] Rodolfo A. Jalabert, A. Douglas Stone and Y. Alhasid, 1992, Statistical Theory of Coulomb-Blockade Oscillation: Quantum Chaos in Quantum Dots, Phys. Rev. Lett 23., 68, 3468.
[24] Y. Meir, N. Wingreen, and P. A. Lee, 1991, Transport Through a Strongly Interacting Electron System: Theory of Periodic Conductance Oscillations, Phys. Rev. Lett. 66, 3048.
[25] T.A.Brody, J.Flores, J.B.French, P.A.Mello, A.Pandey and S.S.M. Wong, 1981, Random-Matrix Physics: Spectrum and Strength Fluctuations, Rev. Mod. Phys. 53, 385.
[26] Y. Alhassid, J. N. Hormuzdiar, and N. Whelan, 1998, Coulomb-Blockade Conductance Peak Distributions in Quantum Dots and the Crossover between Orthogonal and Unitary Symmetry, Phys. Rev. B 55, 4866.
[27] P. Shukla, 2007, Eigenfunction Statistics of Complex Systems: A Common Mathematical Formulation, Phys. Rev. E 75, 051113.
[28] Y. Alhassid, C. H. Lewenkopf, 1995, Statistical Distributions of Level Widths and Conductance Peaks in Irregularly Shaped Quantum Dots, Phys. Rev. Lett. 75, 3922.